

Quantum states of muons in fluorides

J. S. Möller,^{1,*} D. Ceresoli,² T. Lancaster,³ N. Marzari,⁴ and S. J. Blundell¹

¹*Department of Physics, Clarendon Laboratory, Oxford University, Parks Road, Oxford OX1 3PU, UK*

²*Istituto di Scienze e Tecnologie Molecolari CNR, via Golgi 19, 20133 Milano, Italy*

³*Centre for Materials Physics, Durham University, South Road, Durham DH1 3LE, UK*

⁴*Theory and Simulation of Materials (THEOS), École Polytechnique Fédérale de Lausanne, 1015 Lausanne, Switzerland*

(Received 23 December 2012; published 18 March 2013)

Muon-spin relaxation (μ^+ SR) is a sensitive probe of magnetism, but its utility can be severely limited by the lack of knowledge of the muon implantation site and the extent to which the muon perturbs its host. We demonstrate systematically that these problems can be addressed accurately using electronic-structure calculations. We show that diamagnetic muons introduce significant short-ranged distortions in ionic insulators that would lead to systematic errors on magnetic moments determined by μ^+ SR, and quantify these. The F- μ -F complex formed by muons in many fluorides can be understood as an exotic molecule-in-a-crystal defect with a zero-point energy larger than that of any naturally occurring triatomic molecule.

DOI: 10.1103/PhysRevB.87.121108

PACS number(s): 76.75.+i, 71.15.Mb, 75.25.-j

Muon-spin relaxation (μ^+ SR) involves implanting spin-polarized positive muons in a sample in order to probe the local magnetic structure.¹ μ^+ SR is an extremely sensitive probe of magnetism² but has two significant limitations. The first concerns the lack of knowledge of the site of implantation of the muon, which hinders the measurement of magnetic moments using μ^+ SR. Second, the unknown extent of the perturbation due to the muon of the local crystal and electronic structure of the host has been the cause for increased concern since μ^+ SR is frequently employed in the study of systems that lie on the verge of ordering²⁻⁵ or where doping is a critical parameter.⁶⁻⁸ Previous first-principles studies have focused on the paramagnetic states formed by muons and protons in semiconductors.⁹⁻¹¹ Diamagnetic muon states (where the contact hyperfine coupling is negligible) have received considerably less attention, in spite of their greater utility in the study of magnetic materials. Here we present a detailed microscopic study based on density-functional theory (DFT) of the dia- and paramagnetic muon states in a series of fluorides, where detailed information about the geometry of the diamagnetic muon site is experimentally accessible, enabling an accurate comparison with first-principles predictions.

In host compounds containing fluorine, diamagnetic muons can couple strongly to the fluoride ions often forming linear F- μ -F complexes,¹² although bent F- μ -F and F- μ geometries have been shown to exist as well.¹³ The magnetic dipolar coupling between muon and fluorine nuclear spin gives rise to a signal that is sensitive to the geometry of the muon-fluorine state, allowing an accurate experimental determination of the muon's local site geometry.^{12,13} In the series of nonmagnetic ionic insulators LiF and NaF (rocksalt structure, $a = 4.03$ Å and 4.78 Å), CaF₂ and BaF₂ (fluorite structure, $a = 5.46$ Å and 6.20 Å), and for the antiferromagnetic insulator CoF₂ (rutile-type structure, $a = 4.70$ Å and $c = 3.18$ Å), we demonstrate the high accuracy with which quantitative information about the muon both in the dia- and the paramagnetic state can be obtained with DFT. We show that diamagnetic muons cause significant short-ranged perturbations of the host, not limited to the fluorides bound in the F- μ -F state (indeed the distortion of the neighboring cations can exceed that of the fluorides).

This introduces systematic errors on magnetic moments in ionic insulators determined by μ^+ SR, which we quantify. We study the quantum behavior of the muon and the heavier proton in both charge states.

The *ab initio* calculations were performed with the QUANTUM ESPRESSO package.¹⁴ Unless indicated otherwise, calculations were performed in a supercell containing $2 \times 2 \times 2$ conventional unit cells. The charge state of the muon was determined by the charge of the supercell (+1 for diamagnetic and neutral for paramagnetic states). A muon was placed in several randomly chosen low-symmetry sites and all ions were allowed to relax until the forces on all ions and the energy change had fallen below a convergence threshold.¹⁵

We first discuss the equilibrium geometries of the muon states obtained from our calculations, shown in Fig. 1. Our results predict the formation of diamagnetic linear F- μ -F states in all of the compounds of this series. This is in agreement with previous experimental data for nonmagnetic LiF, NaF, CaF₂, and BaF₂.¹² The calculated and experimentally measured bond lengths are tabulated in Table I. Our calculated bond lengths are in all cases within 3% of the experimental values demonstrating the high level of accuracy of these results. We have found no evidence for any other stable diamagnetic states in this series. For CoF₂ a detailed experimental study¹⁶ has determined the muon site to be the octahedral $\frac{1}{2}00$ site, in agreement with our calculations, although no experimental reports of an F- μ -F state exist. In that experiment,^{16,17} the paramagnetic region, where a potential F- μ -F signal would be present, was studied only under an applied magnetic field, impeding the observation of a potential F- μ -F signal. Following our first-principles results, we have therefore searched for experimental signatures of an F- μ -F state in CoF₂ in zero applied field. We have found unambiguous experimental evidence¹⁵ for a symmetric, linear F- μ -F state with a fluoride-fluoride separation of $2.43(2)$ Å, in good agreement with our calculated value of 2.36 Å. These results demonstrate that DFT is a powerful tool for determining diamagnetic muon sites.

Using a supercell approach, we can also quantify the extent of the perturbation of the implanted muon on its host. The

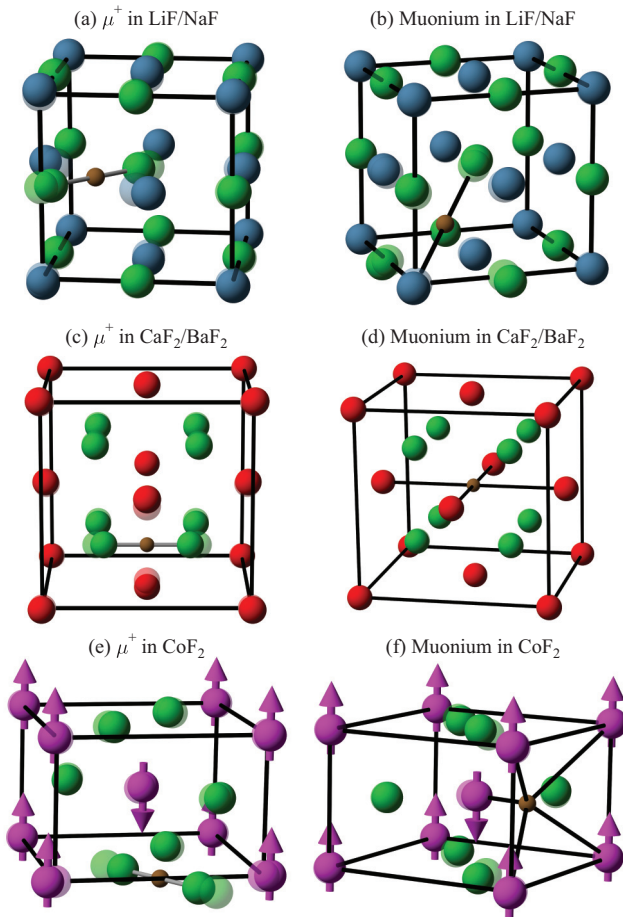


FIG. 1. (Color online) Calculated equilibrium geometries of diamagnetic and paramagnetic muon states in LiF/NaF (Li/Na blue, F green), CaF₂/BaF₂ (Ca/Ba red), and CoF₂ (Co magenta). Translucent spheres represent the equilibrium ionic positions before the muon (brown) is introduced into the crystal. Black lines are a guide to the eye. The *c* axis is vertical.

calculated structures (Fig. 1) allow us to study the radial displacements of the ions as a function of their unperturbed distance from the muon site (Fig. 2). The calculated displacements demonstrate that the muon's perturbation is large but short ranged. While it is known that the perturbation of the fluoride ions must be significant based on the experimentally measured F- μ bond lengths of the F- μ -F states found in many fluorides,^{12,13} we can now quantify the perturbation of the cations as well. Since localized magnetic moments would be located on the cation, the cation displacements are particularly pertinent to understanding the effect of the muon's perturbation on experimentally measured μ^+ SR spectra discussed below. Our results show that in LiF, CaF₂, and BaF₂ the perturbation of the nearest neighbor (n.n.) cations even exceeds those of the fluoride ions bound in the F- μ -F state. At short distances the direct Coulomb interaction between the muon and the surrounding ions dominates over the elastic interaction transmitted through the lattice. We therefore expect similar

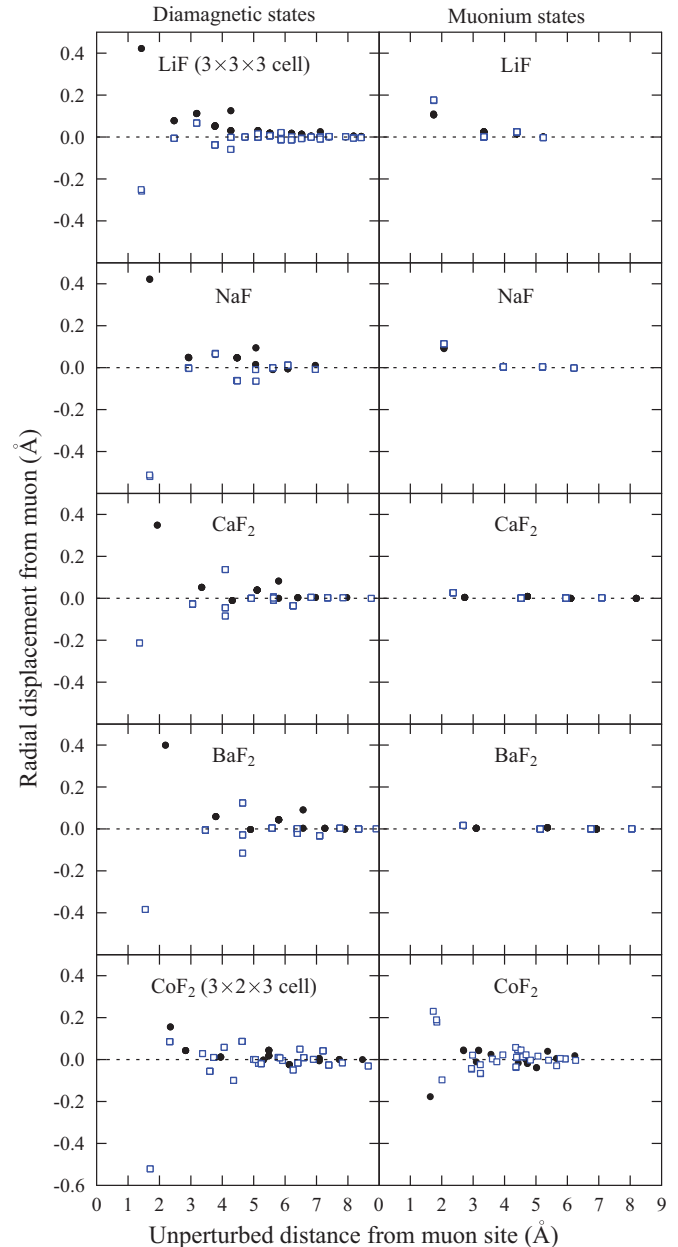


FIG. 2. (Color online) The radial displacements of the ions as a function of their distance from the muon site in the unperturbed crystal. Cation (black circle), fluoride (blue square). For all compounds the displacements are well converged already on a $2 \times 2 \times 2$ supercell but for LiF and CoF₂ the F- μ -F displacements are shown for larger cells.

distortions to be present in *any* ionic insulator, regardless of whether it contains fluoride ions or not. Indeed we believe that the formation of the F- μ -F state somewhat mitigates the n.n. cation distortions due to the attraction of negative charge density towards the muon. At short distances all displacements are radially in- or outwards from the muon due to the symmetry of the site. Beyond the n.n. shell, elastic interactions cause some nonradial displacement.

We have also investigated the effect that the muon has on the magnetic moments of the surrounding ions. In this

series only CoF_2 is magnetic. The spin-only moment was estimated from a Löwdin population analysis to be $2.68\mu_B$ per Co ion. This compares with a total moment of $2.60(4)\mu_B$ measured with powder neutron diffraction²¹ and a spin-only moment of $2.21(2)\mu_B$ determined from high-energy photon diffraction.²² We find the largest perturbation of the Co spin-only moment due to the presence of the *diamagnetic* muon to be about $\pm 0.5\%$ and therefore negligible. We believe that the perturbation of the total moment will be similar and therefore have a negligible effect on experimental μ^+ SR spectra.¹⁵

In a μ^+ SR experiment, a muon at position \mathbf{r}_μ couples to the dipolar field¹⁵ $\mathbf{B}_{\text{dip}}(\mathbf{r}_\mu)$ of the host's magnetic moments. There is negligible contact hyperfine coupling for the diamagnetic F- μ -F muons, so in CoF_2 the F- μ -F muons only probe $\mathbf{B}_{\text{dip}}(\mathbf{r}_\mu)$, which we have calculated for both an unperturbed crystal and an aperiodic perturbed crystal (simulating the presence of the muon).¹⁵ The perturbation of the magnetic moments has been neglected. Our calculations predict a reduction of the dipolar field at the muon site by 21.4% ($2 \times 2 \times 2$ supercell), 23.6% ($3 \times 2 \times 3$ supercell), and 23.9% ($4 \times 2 \times 2$ supercell). Experimentally the dipolar coupling is measured to be 16% lower¹⁶ than expected from a Co moment of $2.64\mu_B$. This is in reasonable agreement with our prediction and demonstrates that relaxed geometries obtained from DFT are suitable for calculating corrections to expected dipolar fields and hence magnetic moments measured by μ^+ SR. Note that the perturbation of the n.n. cations in CoF_2 is fairly moderate in comparison with the other compounds in this series (Fig. 2). Nonetheless the n.n. cation displacements in CoF_2 have a significant effect on the calculated dipolar coupling due to the short-ranged nature of the dipolar interaction.¹⁵ This illustrates that in ionic insulators the muon's perturbation cannot be neglected if magnetic moments are to be measured accurately by μ^+ SR. In more covalent compounds we expect the μ^+ charge to be more screened and so structural distortions are probably smaller.

All of the results above are valid for a positive muon, a proton, or a deuteron defect and are "classical" in the sense that they do not take account of zero-point effects due to the small muon mass ($m_\mu \approx m_p/9$). We have used density-functional perturbation theory²³ (DFPT) to calculate the vibrational properties of the F- μ -F system in the solid and in vacuum (Table I). In vacuum the linear (F- μ -F)⁻ anion has four vibrational modes: symmetric stretch, bending (twofold degenerate), and asymmetric stretch. In the solid the twofold degeneracy of the bending mode is broken due to the symmetry of the site: in LiF, NaF, CaF_2 , and BaF_2 there are two fundamentally inequivalent directions of bending; one is towards a neighboring cation and is shifted up in frequency while the other direction is into a "gap" in the crystal structure and is shifted down in frequency. The asymmetric stretch is very similar to its vacuum value except in CaF_2 , where the small bond length leads to a larger value. In CaF_2 , BaF_2 , and CoF_2 all F- μ -F modes are highly localized and decouple from the lattice modes. The decoupling of the vibrational modes of the linear F- μ -F system illustrates that it may be viewed as a molecule-in-a-crystal defect similar to the V_K center found in the alkali halides.²⁴ In LiF and NaF the symmetric stretch mode mixes with the lattice modes so this analogy is slightly less

TABLE I. Calculated (DFT) and experimental (exp) properties of the diamagnetic F- μ -F states in solid and vacuum, and of the (FHF)⁻ molecular ion in vacuum. r (Å) is the muon-fluoride bond length, ν is the frequency (cm^{-1}) of the symmetric stretch (SS), asymmetric stretch (AS), and bending (B) mode, and ZPE is the zero-point energy (eV). ^aOur calculation. ^bExperimental data (Ref. 19). ^cRef. 20 reports 1377 cm^{-1} .

	$2r_{\text{DFT}}$	$2r_{\text{exp}}$	ν_{SS}	ν_{B}	ν_{B}	ν_{AS}	ZPE
(FHF) ^{-a}	2.36	2.28	581	1289	1289	1611	0.30
(FHF) ^{-b}		2.28	583	1286	1286	1331 ^c	0.28
(F- μ -F) ⁻	2.36		581	3797	3797	4748	0.80
LiF	2.34 ¹⁸	2.36(2) ¹²		2825	4603	4881	0.76
NaF	2.35	2.38(1) ¹²		3071	4363	4813	0.76
CaF_2	2.31	2.34(2) ¹²	649	2737	4481	5446	0.83
BaF_2	2.33	2.37(2) ¹²	613	3033	4130	4974	0.79
CoF_2	2.36	2.43(2)	585	3076	3473	4570	0.73

apposite. From the frequencies of the decoupled vibrational modes we have estimated the zero-point energy (ZPE) of the system (in the harmonic approximation). The muon-fluoride (or hydrogen-fluoride) bond is the strongest known hydrogen bond in nature.²⁵ Combined with the small mass of the muon this leads to the exceptionally large ZPE of the F- μ -F center of 0.80 eV in vacuum, which is larger than the ZPE of any natural triatomic molecule (the ZPEs of H_2O and H_3^+ are 0.56 and 0.54 eV, respectively²⁶). This demonstrates the importance of quantum effects in muon localization.

We now discuss the properties of the neutral muonium (Mu) state in this series. The calculated equilibrium geometries are shown in Fig. 1. Since the muon charge is screened by an electron, the Mu site is fundamentally different to the diamagnetic site. In LiF and NaF, Mu occupies the octahedral interstitial site. An interstitial site was previously suggested based on the observed hyperfine coupling.²⁷ In CaF_2 and BaF_2 , Mu occupies the octahedral cation-cation centered site; the fluoride-fluoride centered octahedral site is unstable. In CoF_2 we find a single Mu site in a nearly octahedral position at approximately (0.56, 0.84, 0.50), distorted by the neighboring fluoride. Figure 2 shows the radial displacements of the ions from the Mu defect. Due to the screening effect of the Mu electron, the displacements are generally much smaller than for the diamagnetic μ^+ . In LiF, NaF, CaF_2 , and BaF_2 the displacements of the n.n. ions are again along the radial direction due to the symmetry of the Mu site and the ions are only displaced away from the Mu. In CoF_2 the symmetry of the Mu site is lower, leading to small displacements in the tangential direction, even for the n.n. shell, through elastic interactions with the lattice. These are also the likely cause for the effective attraction of some ions despite the neutral charge state of Mu. All of this also applies to neutral interstitial hydrogen H_i^0 .

The paramagnetic state is experimentally characterized by the (dipolar and contact) hyperfine coupling between the muon (proton) spin and the surrounding spin density. For all paramagnetic states above, except the one in CoF_2 , the dipolar coupling cancels by symmetry. Unlike in the diamagnetic case, the n.n. Co spin-only moment is significantly perturbed

TABLE II. Calculated and experimental contact hyperfine couplings (MHz) and zero-point energies E (eV) of Mu and H defects. A : “classical” hyperfine coupling; $\langle A \rangle$: quantum corrected value using the harmonic approximation (HA), by solving the full Schrödinger equation using finite differences (FD). The ratio of E_{HA} for the Mu and H modes is close to $\sqrt{m_p/m_\mu} \approx 3$ indicating highly localized modes. ^aMeasured (Ref. 33) to be 0.12 eV at 100 K. ^bWhile no experimental value A_{exp} has been reported for CoF₂, a total coupling of 1280 MHz has been measured (Ref. 34) in MnF₂. The dipolar coupling (without quantum correction) in CoF₂ is ≈ 71 MHz (0.52 T along c) and adds to the contact term.

		A	E_{HA}	$\langle A \rangle_{\text{HA}}$	E_{FD}	$\langle A \rangle_{\text{FD}}$	A_{exp}
Vac.	Mu	4711					4463
	H _i ⁰	1480					1420
LiF	Mu	4368	0.50	4256	0.51	4238	4584 ²⁷
	H _i ⁰	1372	0.18	1361	0.17	1360	1400 ²⁸
NaF	Mu	4389	0.38	4293	0.42	4208	4642 ²⁷
	H _i ⁰	1379	0.13	1371	0.14	1367	1500 ²⁹
CaF ₂	Mu	4610	0.31	4564	0.33	4564	4479 ³⁰
	H _i ⁰	1448	0.10 ^a	1440	0.10	1440	1464 ³¹
BaF ₂	Mu	4605	0.20	4560	0.23	4565	
	H _i ⁰	1447	0.07	1440	0.07	1440	1424 ³²
CoF ₂	Mu	1281	0.62	1397	0.59	1535	^b
	H _i ⁰	403	0.21	420	0.20	441	

(−25%) by the presence of the Mu. The estimate of the dipolar coupling assumes that the relative perturbation of the total moment is also −25% and takes account of crystallographic distortions.¹⁵ The contact hyperfine coupling A is related to the unpaired spin density $\rho(\mathbf{r}_n)$ at the muon/proton position \mathbf{r}_n via $A = \frac{2\mu_0}{3} \gamma_e \gamma_n \rho(\mathbf{r}_n)$, where γ_e is the electron gyromagnetic ratio and γ_n is the muon/proton gyromagnetic ratio. The spin density was obtained using the projector-augmented wave reconstruction method³⁵ and the resulting contact hyperfine couplings are shown in Table II. However, due to the ZPE of the defect, the defect wave function has a finite spread leading to a quantum correction to the hyperfine coupling. This has been previously studied in Si, Ge, and diamond.^{10,11} Although a complete treatment would involve a parametrization of the full three-dimensional contact hyperfine coupling and potential energy surface to calculate the three-dimensional wave function,¹⁰ we obtain an estimate of this correction as follows. The vibrational modes of the defect were calculated using DFPT and the potential energy and hyperfine coupling were calculated along the direction of the eigenmodes. Since the eigenmodes are mutually perpendicular, the motion along the three modes decouples and the wave function factorizes. We have then calculated the Mu and H_i⁰ wave functions in two ways. The first is an anisotropic harmonic approximation where the wave function along each mode is the ground-state wave function of the harmonic oscillator with the frequency ω given by the calculated vibrational frequency. Inspection of the potential energy surface has revealed significant anharmonic terms along some directions in some of the compounds.¹⁵ We have therefore also solved the full Schrödinger equation along the calculated mode directions using a finite-differences method. From the calculated contact hyperfine couplings $A(\mathbf{r})$

and the Mu/H_i⁰ wave function $\psi(\mathbf{r})$, we have obtained the estimated quantum correction $\langle A \rangle$ from $\langle A \rangle = \frac{\int r^2 dr |\psi(\mathbf{r})|^2 A(\mathbf{r})}{\int r^2 dr |\psi(\mathbf{r})|^2}$. The calculated couplings $A(\mathbf{r})$ and wave function $\psi(\mathbf{r})$ are weighted by r^2 to obtain an approximate three-dimensional average. This approximation is accurate so long as $\psi(\mathbf{r})$ and $A(\mathbf{r})$ are approximately spherically symmetric between neighboring points on the integration grid. Since the average is taken over three mutually perpendicular directions, we expect this to be a reasonable approximation. The quantum corrections are also tabulated in Table II. Note that this correction is smaller for the heavier H_i⁰. Our estimates are within 10% of the experimental value for LiF and NaF, the same level of accuracy as previous calculations in Si, Ge, and diamond,^{10,11} and within 2% of the experimental value for CaF₂.

There has been considerable interest recently in identifying muon sites by locating the minima of the electrostatic potential of the unperturbed host.^{36–40} We have therefore compared the muon sites in this series with the location of the minima of the electrostatic potential of the unperturbed solid, and have found that these do not generally coincide.^{15,18} In the diamagnetic case this is primarily due to the formation of the molecular F- μ -F state. While interstitial Mu interacts more weakly with the host due to the screening by the Mu electron, this screening also makes Mu less sensitive to the host’s electrostatic potential and the Mu site is mainly determined by the space required to accommodate the Mu electron. All of the compounds studied here are very ionic in character and the μ^+ -lattice interaction is therefore expected to be stronger than in more covalent insulators or metals (where the μ^+ charge would at least be partially screened). Nonetheless we expect the combination of this screening (where operative), the muon-lattice interaction, and the muon’s exceptionally large zero-point energy to frequently lead to muon localization away from the minima of the electrostatic potential of the unperturbed host. We therefore believe that muon sites cannot be determined reliably on the basis of the electrostatic potential alone.

In conclusion we have demonstrated systematically how DFT can be used to comprehensively address the two most fundamental limitations of the μ^+ SR technique: the problem of the unknown muon site and the perturbation exerted by the muon on its host. We note that the detailed understanding of the nature of the muon’s state in solids is relevant beyond the field of μ^+ SR since the muon acts as a light analog of hydrogen, which is a ubiquitous impurity in all technologically important semiconductors, where it strongly affects the electronic and structural properties of the material.⁴¹

We thank the following people for useful discussions and technical help: Pietro Bonfà, Roberto De Renzi, Fabio Bernardini, Nikitas Gidopoulos, Fan Xiao, Jack Wright, Andrew Steele, Andrea Dal Corso, Emine Küçükbenli, Bill Hayes, and Steve Cox. Calculations were performed on computers of the E-Infrastructure South Initiative (UK), the Très Grand Centre de calcul (France), CINECA (Italy), and EPFL (Switzerland). The muon experiment on CoF₂ was performed on the GPS instrument at the Paul-Scherrer Institut, Villigen, Switzerland. This work is supported by EPSRC (UK).

*johannes.moeller@physics.ox.ac.uk

- ¹S. J. Blundell, *Contemp. Phys.* **40**, 175 (1999).
- ²F. L. Pratt, P. J. Baker, S. J. Blundell, T. Lancaster, S. Ohira-Kawamura, C. Baines, Y. Shimizu, K. Kanoda, I. Watanabe, and G. Saito, *Nature (London)* **471**, 612 (2011).
- ³K. Kojima, A. Keren, G. M. Luke, B. Nachumi, W. D. Wu, Y. J. Uemura, M. Azuma, and M. Takano, *Phys. Rev. Lett.* **74**, 2812 (1995).
- ⁴T. Lancaster, S. J. Blundell, M. L. Brooks, P. J. Baker, F. L. Pratt, J. L. Manson, C. P. Landee, and C. Baines, *Phys. Rev. B* **73**, 020410 (2006).
- ⁵S. J. Blundell, F. L. Pratt, P. A. Pattenden, M. Kurmoo, K. H. Chow, S. Takagi, T. Jestädt, and W. Hayes, *J. Phys.: Condens. Matter* **9**, L119 (1997).
- ⁶E. Amit and A. Keren, *Phys. Rev. B* **82**, 172509 (2010).
- ⁷G. M. Luke *et al.*, *Phys. Rev. B* **42**, 7981 (1990).
- ⁸J. D. Wright *et al.*, *Phys. Rev. B* **85**, 054503 (2012).
- ⁹C. G. Van de Walle, *Phys. Rev. Lett.* **85**, 1012 (2000).
- ¹⁰A. R. Porter, M. D. Towler, and R. J. Needs, *Phys. Rev. B* **60**, 13534 (1999).
- ¹¹R. H. Luchsinger, Y. Zhou, and P. F. Meier, *Phys. Rev. B* **55**, 6927 (1997).
- ¹²J. H. Brewer, S. R. Kreitzman, D. R. Noakes, E. J. Ansaldo, D. R. Harshman, and R. Keitel, *Phys. Rev. B* **33**, 7813 (1986).
- ¹³T. Lancaster, S. J. Blundell, P. J. Baker, M. L. Brooks, W. Hayes, F. L. Pratt, J. L. Manson, M. M. Conner, and J. A. Schlueter, *Phys. Rev. Lett.* **99**, 267601 (2007).
- ¹⁴P. Giannozzi *et al.*, *J. Phys.: Condens. Matter* **21**, 395502 (2009).
- ¹⁵See Supplemental Material at <http://link.aps.org/supplemental/10.1103/PhysRevB.87.121108> for more details.
- ¹⁶R. De Renzi, G. Guidi, P. Podini, R. Tedeschi, C. Bucci, and S. F. J. Cox, *Phys. Rev. B* **30**, 186 (1984).
- ¹⁷R. De Renzi, G. Guidi, P. Podini, R. Tedeschi, C. Bucci, and S. F. J. Cox, *Phys. Rev. B* **30**, 197 (1984).
- ¹⁸This is in agreement with a recent independent study on LiF and YF₃: F. Bernardini, P. Bonfà, S. Massidda, and R. De Renzi, [arXiv:1302.2031](https://arxiv.org/abs/1302.2031).
- ¹⁹K. Kawaguchi and E. Hirota, *J. Chem. Phys.* **87**, 6838 (1987).
- ²⁰R. D. Hunt and L. Andrews, *J. Chem. Phys.* **87**, 6819 (1987).
- ²¹W. Jauch, M. Reehuis, and A. J. Schultz, *Acta Crystallogr. A* **60**, 51 (2004).
- ²²J. Stempffer, U. Rütt, S. P. Bayrakci, T. Brückel, and W. Jauch, *Phys. Rev. B* **69**, 014417 (2004).
- ²³S. Baroni, S. de Gironcoli, A. Dal Corso, and P. Giannozzi, *Rev. Mod. Phys.* **73**, 515 (2001).
- ²⁴W. Hayes and A. M. Stoneham, *Defects and Defect Processes in Nonmetallic Solids* (Dover, New York, 2004).
- ²⁵G. A. Geoffrey, *An Introduction to Hydrogen Bonding* (Oxford University Press, 1997).
- ²⁶G. D. Carney and R. N. Porter, *J. Chem. Phys.* **65**, 3547 (1976).
- ²⁷H. Baumeler *et al.*, *Hyperfine Interact.* **32**, 659 (1986).
- ²⁸T. Kamikawa, *Phys. Status Solidi B* **99**, 721 (1980).
- ²⁹C. Hoentzsch and J. Spaeth, *Solid State Commun.* **29**, 577 (1979).
- ³⁰R. F. Kiefl, E. Holzschuh, H. Keller, W. Kündig, P. F. Meier, B. D. Patterson, J. W. Schneider, K. W. Blazey, S. L. Rudaz, and A. B. Denison, *Phys. Rev. Lett.* **53**, 90 (1984).
- ³¹J. L. Hall and R. T. Schumacher, *Phys. Rev.* **127**, 1892 (1962).
- ³²J. W. Hodby, *J. Phys. C: Solid State* **2**, 404 (1969).
- ³³R. E. Shamu, W. M. Hartmann, and E. L. Yasaitis, *Phys. Rev.* **170**, 822 (1968).
- ³⁴R. F. Kiefl, G. M. Luke, S. R. Kreitzman, M. Celio, R. Keitel, J. H. Brewer, D. R. Noakes, Y. J. Uemura, A. M. Portis, and V. Jaccarino, *Phys. Rev. B* **35**, 2079 (1987).
- ³⁵P. E. Blöchl, *Phys. Rev. B* **50**, 17953 (1994).
- ³⁶H. Luetkens, M. Stingaciu, Y. G. Pashkevich, K. Conder, E. Pomjakushina, A. A. Gusev, K. V. Lamonova, P. Lemmens, and H.-H. Klauss, *Phys. Rev. Lett.* **101**, 017601 (2008).
- ³⁷H. Maeter *et al.*, *Phys. Rev. B* **80**, 094524 (2009).
- ³⁸M. Bendele, A. Ichsanow, Y. Pashkevich, L. Keller, T. Strässle, A. Gusev, E. Pomjakushina, K. Conder, R. Khasanov, and H. Keller, *Phys. Rev. B* **85**, 064517 (2012).
- ³⁹R. De Renzi *et al.*, *Supercond. Sci. Technol.* **25**, 084009 (2012).
- ⁴⁰G. Prando *et al.*, *Phys. Rev. B* **87**, 064401 (2013).
- ⁴¹C. G. Van de Walle and J. Neugebauer, *Nature (London)* **423**, 626 (2003).